

Coupling of α -channeling to $|k_{\parallel}|$ upshift in lower hybrid current drive

I. E. Ochs,¹ N. Bertelli,² and N. J. Fisch^{3,2}

¹*Department of Physics, Harvard University, Cambridge, Massachusetts 02138*

²*Princeton Plasma Physics Laboratory, Princeton, New Jersey 08543*

³*Department of Astrophysical Sciences, Princeton University, Princeton, New Jersey 08540*

(Dated: April 30, 2022)

Although lower hybrid waves have been shown to be effective in driving plasma current in present-day tokamaks, they are predicted to strongly interact with the energetic α particles born from fusion reactions in eventual tokamak reactors. In the presence of the expected strong α particle birth gradient, however, this interaction can produce wave amplification rather than wave damping, but only if the launch position and orientation of the waveguides are suitably arranged. The flexibilities in achieving the amplification effect are identified through a consideration of symmetries in the channeling effect, in the wave propagation, and in the tokamak field configuration. Interestingly, for current drive that supports the poloidal magnetic field, the achievement of wave amplification through α channeling is fundamentally coupled to effects leading to the elusive $|k_{\parallel}|$ upshift.

PACS numbers: 52.35.-g, 52.55.Fa, 52.55.Wq, 52.55.-s

Introduction: Lower hybrid (LH) waves are predicted to be effective in driving substantial plasma current in tokamaks [1], an effect that has enjoyed extensive demonstration in tokamak experiments [2]. Yet there remains a concern that, in extrapolating to a fusion reactor, high-energy α particles born in the plasma core could strongly damp the LH wave [3, 4]. However, by coupling diffusion in energy to diffusion in space (known as *alpha channeling*), a favorable population inversion may appear along the diffusion path, causing the α particles to amplify rather than damp the wave [5].

The possibilities in exploiting this effect are now made urgent by recent interesting suggestions featuring launching from the tokamak high-field side [6], with extrapolations to the proposed ARC tokamak reactor [7]. This so-called “inside launch” approach is thought to make the LH wave more able to penetrate the plasma core, while better protecting the waveguide from the plasma. While there have been many ray-tracing studies of LH waves to optimize the current drive effect in existing and planned devices [8–20], no study has taken into account how launch position can minimize α -particle damping were the wave to penetrate close to the plasma center of a reactor where α -particles would be abundant. Thus, the questions posed and answered here are the following: If the inside launch approach is employed, then how can the interactions with high-energy α particles be made favorable? Which launch parameters for the LH wave avoid or reverse the α -particle damping rather than exacerbate it? How large must the spatial gradients in the α -particle birth distribution be to reverse the the damping effect?

The channeling effect depends crucially on the sign of poloidal wavenumber k_{θ} [5]. This dependency was exploited in the channeling effect for ion Bernstein waves [21], where particularly large wavenumbers could be arranged as a result of mode conversion, rendering this wave highly suitable for large channeling effects [22]. In

the case of the LH wave, k_{θ} is a function both of the launch geometry and the position along the ray [23]. Also, for the LH wave, in the wave interaction with α particles k_{θ} determines the channeling condition, whereas in the interaction with electrons, the toroidal wavenumber k_{ϕ} , determines the current drive direction. These features of the LH wave constrain the possibilities in achieving simultaneously both amplification and current drive.

The flexibilities in achieving both these effects with the LH wave are found by a consideration of the symmetries in the channeling effect, in the wave propagation, and in the tokamak field configuration. Numerical simulations of LH rays give the optimum launch positions and grill orientations and also confirm these symmetries. What we find is that, for current drive supporting the poloidal magnetic field and for $B_{\phi} > 0$, the ray should be launched from $210^{\circ} < \theta < 300^{\circ}$, with a grill orientation that results in $k_{\theta} > 0$, where the poloidal angle θ is measured counterclockwise from the low-field side equator, and the toroidal angle ϕ is measured counterclockwise around the torus when viewed from the top.

We also find that there is an inescapable coupling of α -channeling to the so-called “ $|k_{\parallel}|$ upshift”, where k_{\parallel} is the wavenumber parallel to the magnetic field. This upshift is thought to resolve the so-called “spectral gap” puzzle in LH wave interactions [24]. Since the phase velocity of injected waves appears to be too high to interact with electrons, only an upshift in $|k_{\parallel}|$ along the ray will produce a resonance. The upshift itself, while well documented experimentally [25–27], continues to elude definitive explanation. The coupling constrains the flexibilities in achieving the α -channeling effect, but still leaves room for favorable conditions. Interestingly, we find that an upshift must occur for LH waves that both support the channeling effect and drive current supportive of the poloidal magnetic field.

Fundamental Constraints: To see how the channeling

direction is constrained under LH wave propagation, consider first that α particles that gain energy from the interaction move in the direction of $\mathbf{k} \times \mathbf{B}$, while those that lose energy move in the direction of $-\mathbf{k} \times \mathbf{B}$ (Fig. 1a). For “proper” α channeling, the α particles that gain energy move to the plasma center. Consider a tokamak with circular magnetic surfaces, so that the flux surface normal vector is given by $\hat{\mathbf{r}}$, the minor radius vector of the torus. Of interest then is the sign and magnitude of $\xi \equiv \frac{\mathbf{k} \times \mathbf{B}}{|\mathbf{k} \times \mathbf{B}|} \cdot \hat{\mathbf{r}}$. The magnitude of ξ represents the extent to which particles are pushed in the radial direction, while the sign represents the direction of channeling: when negative, particles that gain energy will be pushed to the plasma center. Thus ξ must be negative to reduce or reverse the damping. Since $|B_\phi| \gg |B_\theta|$ and $k_\perp \gg k_\parallel$, it follows that

$$\xi \equiv \frac{\mathbf{k} \times \mathbf{B}}{|\mathbf{k} \times \mathbf{B}|} \cdot \hat{\mathbf{r}} \approx -\frac{k_\theta}{|k_\perp|} \quad (1)$$

where $|k_\perp| = \sqrt{k_\theta^2 + k_r^2}$. Thus, for $B_\phi > 0$, to produce proper channeling requires k_θ to be positive (Figure 1b).

For the LH wave, the sign of k_θ turns out to be intimately connected with the poloidal launch angle: specifically, k_θ tends to decrease along the ray for launch above the poloidal equator ($0^\circ < \theta < 180^\circ$), and increase for launch below it. This effect is *independent of both the direction of current drive and the direction of the magnetic field*. To see how such an effect can arise, we assume a simple, well-known electrostatic model of dispersion for $\Omega_i \ll \omega \ll \Omega_e$ [23]:

$$D_0 \approx (c^2/\omega^2) \left(k_\perp^2 - (\omega_{pe}/\omega)^2 k_\parallel^2 \right) \quad (2)$$

$$B_\phi = \frac{B_{\phi 0}}{1 + \frac{r}{R_0} \cos \theta} \quad (3)$$

Although this model is strictly valid only near $k_\theta = 0$, simulations show that the symmetries uncovered here also hold for the full dispersion relation. For tokamaks, $B_\phi \gg B_\theta$ and $\omega_{pe} \gg \omega$, so that the initial evolution of

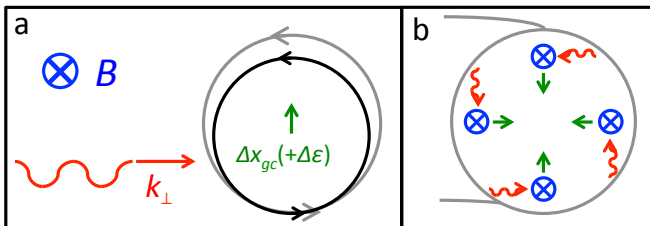


FIG. 1: (a) Schematic of the channeling effect, showing the coupling between Δx and $\Delta \epsilon$. When wave energy is channeled into the particles, they move in the direction of $\mathbf{k} \times \mathbf{B}$. (b) In a tokamak magnetic field configuration, \mathbf{B} (blue) is approximately aligned with the toroidal tangent vector $\hat{\phi}$, and so an inward-pointing $\mathbf{k} \times \mathbf{B}$ (green) requires positive k_θ (red). In this case, $\xi \approx -k_\theta/k_\perp$. Color available online.

k_θ (when $k_\theta \simeq 0$) is determined by

$$\frac{dk_\theta}{dt} = \frac{\partial D_0 / \partial \theta}{\partial D_0 / \partial \omega} \approx - \left(\frac{B_\theta^2}{B_{\phi 0}^2} \right) \left(\frac{\omega^3 (R_0 + r \cos \theta)}{2\omega_{pe}^2 R_0^2} \right) \sin \theta, \quad (4)$$

and

$$\frac{d\theta}{dt} = -\frac{\partial D_0 / \partial m}{\partial D_0 / \partial \omega} \approx \left(\frac{1}{B_{\phi 0}} \right) \left(\frac{B_\theta}{k_\phi} \right) \left(\frac{\omega (R_0 + r \cos \theta)}{2rR_0} \right). \quad (5)$$

For current drive supporting the poloidal magnetic field ($k_\phi B_\theta > 0$), and for proper channeling $k_\theta B_\phi > 0$, it follows that $B_\phi > 0$ requires $dk_\theta/dt > 0$. Now since $dk_\theta/dt \propto -\sin \theta$, the launch should ensue from *below the poloidal equator* to ensure proper channeling.

Eqs. (4) and (5) reveal symmetries of the channeling effect that are confirmed by simulations of the full geometrical optics ray equations (Fig. 2). First, for current drive supportive of the poloidal magnetic field ($k_\phi B_\theta > 0$), the sign of B_θ turns out to have no impact on the poloidal trajectory or the evolution of k_θ . This follows directly from the fact that Eqs. (4) and (5) depend only on B_θ^2 and B_θ/k_ϕ . Thus α -channeling is unaffected under coupled reversal of k_ϕ and B_θ . Second, under B_ϕ reversal, proper channeling requires k_θ reversal as well. Since Eq. (4) depends only on $B_{\phi 0}^2$, it follows that $\sin \theta > 0$, corresponding to launch from above the poloidal equator. Interestingly, this sign reversal in dk_θ/dt ensures that, all other quantities equal, a launch with (k_θ, θ) when $B_\phi > 0$ will have a perfectly antisymmetric poloidal trajectory and k_θ evolution to the launch with $(-k_\theta, -\theta)$ when $B_\phi < 0$, since Eq. (5) also changes sign with B_ϕ (Figs. 2a and 2b).

Consider now that the $|k_\parallel|$ shift is determined by the magnitude and sign of $(k_\theta \cdot B_\theta)(k_\phi \cdot B_\phi) = (k_\theta B_\theta)(k_\phi B_\phi)$. Since for supportive current drive $k_\phi B_\theta > 0$, and for proper channeling $k_\theta B_\phi > 0$, launching to ensure proper channeling gives $|k_\parallel| > 0$ regardless of the magnetic field geometry (Fig. 2d).

These constraints apply only for supportive current drive. However, it is sometimes desirable to apply k_ϕ so that the current drive opposes B_θ ($k_\phi B_\theta < 0$), for example for current profile control. Eqs. (4) and (5) then show that although the sign of dk_θ/dt stays the same, the sign of $d\theta/dt$ is reversed, breaking the antisymmetric evolution we observed under B_ϕ reversal. Interestingly, the trajectory resulting from reversed current drive for proper channeling is symmetric with the trajectory resulting from supportive current drive for improper channeling ($k_\theta B_\phi < 0$). Also, since k_ϕ reverses sign while all other quantities remain the same, reversed current drive results inevitably in a $|k_\parallel|$ downshift. In either event, because the direction of the rf-driven current is fundamentally coupled to the sign of the $|k_\parallel|$ shift, there are fewer flexibilities in optimizing the wave launch.

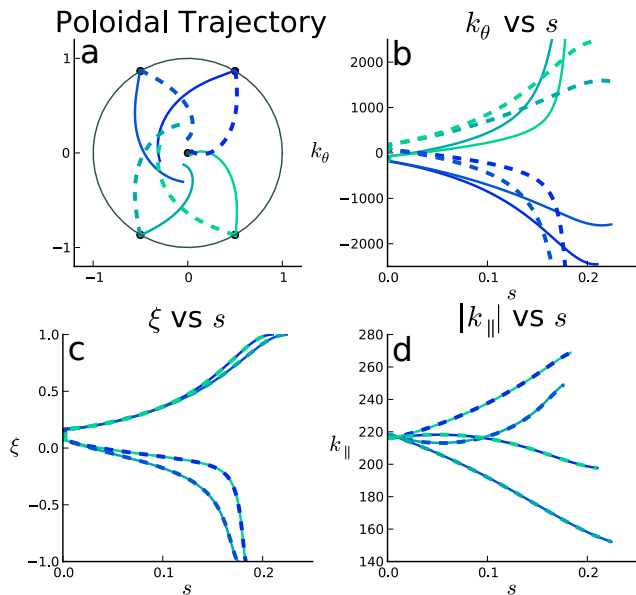


FIG. 2: Simulation results for ray propagation into 5 keV plasma, showing the symmetries with respect to B_ϕ reversal. Solid lines show launches with $(B_\phi > 0, k_\theta > 0)$, while dashed lines show $(B_\phi < 0, k_\theta < 0)$. Reversing B_ϕ , k_θ , and θ results in antisymmetric evolution in θ and k_θ (a-b). The reversals have no effect on ξ or the $|k_\parallel|$ upshift however, which are clearly coupled (c-d). Color available online.

Required α -particle birth gradient: The alpha channeling effect results in diffusion paths in $r - \epsilon_\perp$ (where $\epsilon_\perp = \frac{1}{2}m_\alpha v_\perp^2$) space obeying,

$$\frac{\partial \epsilon_\perp}{\partial r} = \frac{\Delta \epsilon_\perp}{\xi \Delta x_{gc}} = \frac{m_\alpha \Omega_\alpha \omega}{\xi k_\perp} = \frac{Z_\alpha e B \omega}{\xi k_\perp}.$$

For the channeling to amplify, rather than damp, the wave, α particles must be diffused from high energy near the plasma center toward low energy at the plasma periphery. Thus for an α -particle distribution monotonically decreasing in energy at every flux surface, a steep radial gradient in energetic α particles is required to create favorable diffusion conditions. Consider then the smallest α -particle radial gradient that achieves zero damping; any steeper gradient will result in energy being transferred into the wave from the energetic α particles. Zero damping implies a flat phase space density $f(\epsilon_\perp, r)$ along the diffusion paths, or

$$\left(\frac{\partial f}{\partial r} + \frac{\partial f}{\partial \epsilon_\perp} \frac{\partial \epsilon_\perp}{\partial r} = 0 \right)_{v_\perp = \omega/k_\perp}$$

For simplicity, suppose $f(\epsilon_\perp, r)$ is a separable function, $f(\epsilon_\perp, r) = CF(\epsilon_\perp)R(r)$; then it follows that

$$\left[\frac{1}{R} \frac{dR}{dr} = - \left(\frac{1}{F} \frac{dF}{d\epsilon_\perp} \right) \left(\frac{Z_\alpha e B \omega}{\xi k_\perp} \right) \right]_{v_\perp = \omega/k_\perp} \quad (6)$$

The velocity distribution of the α particles is determined assuming the isotropic birth of energetic α

particles from fusion at rate \dot{N}_α . Assuming the LH wave intensities are insufficient to modify the α -particle distribution, then collisions, primarily with electrons, lead, in steady state, to a (three-dimensional) velocity space flux of $\nu v f_v(\mathbf{v})$, where $\nu = 16\sqrt{2\pi}m_e e^4 n_e \times \ln \Lambda / 3T_e^{3/2} m_\alpha \epsilon_0^2$, giving $f(\epsilon_\perp) = \dot{N}_\alpha / 2\nu \epsilon_\perp$. Separating out the radius-dependent and ϵ_\perp -dependent components, we find $F(\epsilon_\perp) = 1/\epsilon_\perp$ and $R(r) = \dot{N}_\alpha X$, where $X \equiv T_e^{3/2} / n_e \log \Lambda$. Using Eq. (6), and noting that the steepness of X is usually much smaller than the required α -particle steepness, we find

$$\chi \equiv \frac{1}{\dot{N}_\alpha} \frac{d\dot{N}_\alpha}{dr} \approx \frac{1}{R} \frac{dR}{dr} = \left(\frac{2Z_\alpha e}{m_\alpha \omega} \right) \left(\frac{k_\perp B}{\xi} \right) \quad (7)$$

This condition gives the steepness in \dot{N}_α (inverse decay length) required for zero damping.

Ray-tracing simulations: Ray-tracing simulations were performed in GENRAY [28], which uses geometrical optics equations and linear electron damping theory [29] to calculate ray trajectories and power absorption. We used a magnetic field configuration file of similar dimensions to the Alcator-C tokamak [26, 30]. The toroidal B field and the plasma current pointed in the $+\phi$ direction, resulting in a $-\theta$ -directed poloidal field.

We simulated one-pass ray trajectories in the absence of α particles, which were then used to determine the α -particle birth steepness χ required for zero damping. Simulated launches were performed with $\omega/2\pi = 4.6$ GHz and with constant $n_t = 2.7$, where n_t was the total refractive index of a specified grill. The poloidal and toroidal refractive indices were then determined by a tilt angle ψ , so that $n_\phi = \pm n_t \cos \psi$ and $n_\theta = n_t \sin \psi$. Radial temperature and density profiles for electrons and ions were given analytically by

$$T(r) = (T_{\max} - T_{\min}) (1 - r^2/a^2) + T_{\min}$$

$$\rho(r) = (\rho_{\max} - \rho_{\min}) (1 - r^2/a^2) + \rho_{\min}$$

where $a = 15.7$ cm was the minor radius of the tokamak, and $T_{\max} = 5$ keV, $T_{\min} = 500$ eV, $\rho_{\max} = 5 \times 10^{19} \text{ m}^{-3}$, and $\rho_{\min} = 10^{19} \text{ m}^{-3}$.

To evaluate the launch positions, we considered three parameters: (i) the average α -particle gradient along the ray required to achieve zero damping; (ii) the radius of closest approach to the plasma core (determined either by the trajectory of entry or by damping on electrons); and (iii) the fraction of the injected power remaining in the ray (undamped on electrons) at the plasma core. An ideal launch should minimize all these quantities.

Results for supportive current drive are shown in Fig. 3. The optimal poloidal launch position clearly falls in the range $210^\circ < \theta < 300^\circ$. Note that launching with an initial $n_\theta > 0$ results in far lower gradient requirements. However, since n_t is fixed under tilting, increasing n_θ too much results in a k_\parallel that is too small to damp on

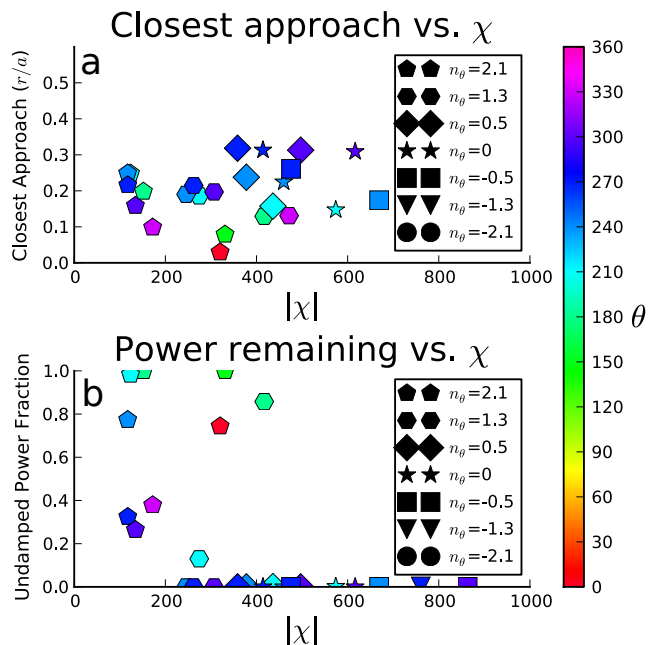


FIG. 3: Supportive current drive simulation results for ray launch with $n_t = 2.7$. Marker shapes indicate initial n_θ , while colors indicate initial poloidal launch point θ . Best launches were from $210^\circ < \theta < 300^\circ$. Increasing the tilt ψ (thus increasing N_θ) decreases $|\chi|$, but too much tilt can downshift k_{\parallel} below the point where the ray can damp on electrons. Color available online.

electrons, as can be seen in Fig. 3b, where 20-95% of the power remains in the ray (unabsorbed) after the initial approach to the plasma core. This effect was especially pronounced for inside launch. Thus, there is a tradeoff between reducing the required gradient and having low enough phase velocity to interact with electrons.

Discussion: Importantly, we can see that LH waves launched from the tokamak's high-field side, which are already predicted to be advantageous from an engineering standpoint [6, 7], can also avoid α -particle damping even as they penetrate near the plasma center. When $B_\phi > 0$ and k_ϕ supports the plasma current, a bottom launch position with a large initial n_θ (achieved by tilting the waveguide away from purely toroidal launch) is optimal for wave amplification. The wave amplification conditions also necessarily result in a $|k_{\parallel}|$ upshift for waves used to support the plasma current, and a $|k_{\parallel}|$ downshift for those used to counteract the plasma current. This coupling to the $|k_{\parallel}|$ shift is a fundamental property.

These results assumed first-pass absorption. However, since the simulations here covered the full range of poloidal launch and tilt, any bouncing off the walls as in multiple-pass absorption are essentially covered insofar as the last bounce would be equivalent to a launch from the last encounter with a wall. Similarly, although they are perhaps useful in avoiding the spectral gap issue, nonlinear effects at the wall [31–36] essentially result in a

launch of a different LH spectrum, also subsumed by the coverage here of all possible launch angles and positions.

We found that the population inversion can only be achieved in the presence of a steep radial α -particle birth gradient, with a decay length on the order of millimeters to a centimeter for Alcator-C-like parameters. For preliminary reactor experiments, the fusion reaction rate will certainly be sharply peaked at the hot plasma center, so the requirement of a peaked α -particle distribution should be easily satisfied. However, we assumed the LH waves were not so strong as to significantly alter the α -particle distribution. Although a reasonable assumption for an experimental tokamak, a reactor in contrast would derive the greatest utility from channeling when much of the energy in the α particles was extracted by the LH wave [37]. In that case, the α particles would not slow down significantly through collisions before being diffused to lower energy by the LH waves. To maintain the appropriate spatial gradients, therefore, a second wave might then be used in addition to the LH wave [38]. Note that the use here of a second wave is essentially different from other uses of a second wave to optimize the current drive efficiency [39–47], since rather than using the second wave to promote interactions with higher velocity electrons, we would use it to facilitate the absorption of energy from the α particles by the LH wave. Both methods should lead to an effective increase in the efficiency.

The potential for alpha channeling to boost reactor efficiency warrants experimental testing. However, the strict symmetries of the channeling effect and its coupling to the $|k_{\parallel}|$ upshift make the predictions here difficult to test directly. After all, the easiest differential test would have been to leave all other parameters equal, but just to reverse k_θ , with one sign giving α -particle damping and the other giving α -particle growth. However, as derived here, the strict coupling of k_θ to the $|k_{\parallel}|$ upshift renders this experiment impossible. In light of this, the best differential test we can hope for is to fix the wave conditions suitable for the channeling effect, but in one case to do so in the presence of an energetic beam of ions, and in the other case in the absence of such a beam. A similar differential test using neutral beams was performed successfully to test channeling effects predicted for the ion Bernstein wave [48].

Conclusions: In sum, the calculations here give a preferred method of launch for LH waves supportive of the plasma current in the presence of α particles, particularly in connection to inside launch approaches. The symmetries uncovered reveal the flexibilities and constraints on both optimizing and experimentally testing the effect.

This work was performed under U.S. DOE contract DE-AC02-09CH11466. One of us (IEO) thanks the support of the National Undergraduate Fellowship Program in Plasma Physics and Fusion Energy Sciences.

-
- [1] N. J. Fisch, *Physical Review Letters* **41**, 873 (1978).
- [2] N. J. Fisch, *Rev. Mod. Phys.* **59**, 175 (1987).
- [3] K. L. Wong and M. Ono, *Nuclear Fusion* **24**, 615 (1984).
- [4] N. J. Fisch and J. M. Rax, *Nuclear Fusion* **32**, 549 (1992).
- [5] N. J. Fisch and J.-M. Rax, *Phys. Rev. Lett.* **69**, 612 (1992).
- [6] Y. A. Podpaly, G. M. Olynyk, M. L. Garrett, P. T. Bonoli, and D. G. Whyte, *Fusion Engineering and Design* **87**, 215 (2012).
- [7] B. Sorbom, J. Ball, T. Palmer, F. Mangiarotti, J. Sierchio, P. Bonoli, C. Kasten, D. Sutherland, H. Barnard, C. Haakonsen, et al., *Fusion Engineering and Design* (submitted) (2014).
- [8] F. Imbeaux and Y. Peysson, *Plasma Phys. Control. Fusion* **47**, 2041 (2005).
- [9] J. Decker, Y. Peysson, J. Hillairet, J. F. Artaud, V. Basiuk, A. Becoulet, A. Ekedahl, M. Goniche, G. T. Hoang, F. Imbeaux, et al., *Nuclear Fusion* **51**, 073025 (2011).
- [10] Y. Peysson and J. Decker, *Fusion Science and Technology* **65**, 22 (2014).
- [11] S. Ceccuzzi, E. Barbato, A. Cardinali, C. Castaldo, R. Cesario, M. Marinucci, F. Mirizzi, L. Panaccione, G. L. Ravera, F. Santini, et al., *Fusion Science and Technology* **64**, 748 (2013).
- [12] W. Horton, M. Goniche, Y. Peysson, J. Decker, A. Ekedahl, and X. Litaudon, *Physics of Plasmas* **20**, 112508 (2013).
- [13] J. Hillairet, D. Voyer, A. Ekedahl, M. Goniche, M. Kazda, O. Meneghini, D. Milanesio, and M. Preynas, *Nuclear Fusion* **50**, 125010 (2010).
- [14] E. Nilsson, J. Decker, Y. Peysson, J. F. Artaud, A. Ekedahl, J. Hillairet, T. Aniel, V. Basiuk, M. Goniche, F. Imbeaux, et al., *Nuclear Fusion* **53**, 083018 (2013).
- [15] S. Xingjian, H. Yemin, and G. Zhe, *Plasma Science & Technology* **14**, 215 (2012).
- [16] M. Schneider, L.-G. Eriksson, F. Imbeaux, and J. Artaud, *Nuclear Fusion* **49**, 125005 (2009).
- [17] M. Spada, M. Bornatici, and F. Engelmann, *Nuclear Fusion* **31**, 447 (1991).
- [18] E. Barbato and F. Santini, *Nuclear Fusion* **31**, 673 (1991).
- [19] E. Barbato and A. Saveliev, *Plasma physics and controlled fusion* **46**, 1283 (2004).
- [20] P. Bonoli and M. Porkolab, *Nuclear fusion* **27**, 1341 (1987).
- [21] N. J. Fisch, *Phys. Plasmas* **2**, 2375 (1995).
- [22] E. J. Valeo and N. J. Fisch, *Phys. Rev. Lett.* **73**, 3536 (1994).
- [23] P. T. Bonoli and E. Ott, *Physics of Fluids* (1958-1988) **25**, 359 (1982).
- [24] P. T. Bonoli and R. C. Englade, *Physics of Fluids* **29**, 2937 (1986).
- [25] S. Bernabei et al., *Phys. Rev. Lett.* **49**, 1255 (1982).
- [26] M. Porkolab, J. J. Schuss, B. Lloyd, Y. Takase, S. Texter, P. Bonoli, C. Fiore, R. Gandy, D. Gwinn, B. Lipschultz, et al., *Physical Review Letters* **53**, 450 (1984).
- [27] C. F. F. Karney, N. J. Fisch, and F. C. Jobes, *Physical Review A* **32**, 2554 (1985).
- [28] A. Smirnov and R. Harvey, *CompX Report CompX-2000-01* (2001).
- [29] P. T. Bonoli, *IEEE Transactions on Plasma science* **12**, 95 (1984).
- [30] M. Porkolab, B. Lloyd, Y. Takase, P. Bonoli, C. Fiore, R. Gandy, R. Granetz, D. Griffin, D. Gwinn, B. Lipschultz, et al., *Physical Review Letters* **53**, 1229 (1984).
- [31] R. Cesario, A. Cardinali, C. Castaldo, F. Paoletti, and D. Mazon, *Physical review letters* **92**, 175002 (2004).
- [32] R. Cesario, L. Amicucci, A. Cardinali, C. Castaldo, M. Marinucci, L. Panaccione, F. Santini, O. Tudisco, M. L. Apicella, G. Calabro, et al., *Nature Communications* **1** (2010).
- [33] A. Zhao and Z. Gao, *Nuclear Fusion* **53**, 083015 (2013).
- [34] N. Bertelli, G. Wallace, P. Bonoli, R. Harvey, A. Smirnov, S. Baek, R. Parker, C. Phillips, E. Valeo, J. Wilson, et al., *Plasma Physics and Controlled Fusion* **55**, 074003 (2013).
- [35] S. Baek, S. Shiraiwa, R. Parker, P. Bonoli, E. Marmor, G. Wallace, A. Dominguez, G. Kramer, and C. Lau, *Physics of Plasmas* **21**, 012506 (2014).
- [36] S. Baek, R. Parker, S. Shiraiwa, G. Wallace, P. Bonoli, D. Brunner, I. Faust, A. Hubbard, B. LaBombard, and M. Porkolab, *Plasma Physics and Controlled Fusion* **55**, 052001 (2013).
- [37] N. J. Fisch and M. C. Herrmann, *Nucl. Fusion* **34**, 1541 (1994).
- [38] N. J. Fisch and M. C. Herrmann, *Nuclear Fusion* **35**, 1753 (1995).
- [39] I. Fidone, G. Giruzzi, G. Granata, and R. Meyer, *Physics of Fluids* **27**, 2468 (1984).
- [40] I. Fidone, G. Giruzzi, V. Krivenski, E. Mazzucato, and L. Ziebell, *Nuclear Fusion* **27**, 579 (1987).
- [41] R. Dumont and G. Giruzzi, *Physics of Plasmas* **11**, 3449 (2004).
- [42] G. Giruzzi, J. Artaud, R. Dumont, F. Imbeaux, P. Bibet, G. Berger-By, F. Bouquey, J. Clary, C. Darbos, A. Ekedahl, et al., *Physical review letters* **93**, 255002 (2004).
- [43] P. Rosa and L. Ziebell, *Plasma Phys. Control. Fusion* **44**, 2065 (2002).
- [44] D. Farina and R. Pozzoli, *Physics of Fluids B* **1**, 815 (1989).
- [45] Y. Dnestrovskij, D. Kostomarov, A. Lukyanitsa, V. Parail, and A. Smirnov, *Nuclear Fusion* **28**, 267 (1988).
- [46] S. Y. Chen, B. B. Hong, Y. Liu, W. Lu, J. Huang, C. J. Tang, X. T. Ding, X. J. Zhang, and Y. J. Hu, *Plasma Physics and Controlled Fusion* **54**, 115002 (2012).
- [47] J. Huang, S. Y. Chen, and C. J. Tang, *Physics of Plasmas* **21**, 012508 (2014).
- [48] D. S. Clark and N. J. Fisch, *Phys. Plasmas* **7**, 2923 (2000).